

RSC Advances



This is an *Accepted Manuscript*, which has been through the Royal Society of Chemistry peer review process and has been accepted for publication.

Accepted Manuscripts are published online shortly after acceptance, before technical editing, formatting and proof reading. Using this free service, authors can make their results available to the community, in citable form, before we publish the edited article. This *Accepted Manuscript* will be replaced by the edited, formatted and paginated article as soon as this is available.

You can find more information about *Accepted Manuscripts* in the [Information for Authors](#).

Please note that technical editing may introduce minor changes to the text and/or graphics, which may alter content. The journal's standard [Terms & Conditions](#) and the [Ethical guidelines](#) still apply. In no event shall the Royal Society of Chemistry be held responsible for any errors or omissions in this *Accepted Manuscript* or any consequences arising from the use of any information it contains.

Cytotoxic 2, 4-Linked Sesquiterpene Lactone Dimers from *Carpesium faberi* Exhibiting NF- κ B Inhibitory Activity

Received 00th January 20xx,
Accepted 00th January 20xx

Yong-xun Yang,^a Shuang Gao,^a Shou-de Zhang,^b Xian-peng Zu,^a Yun-heng Shen,^a Lei Shan,^a Hui-liang Li*^a and Wei-dong Zhang*^{abc}

DOI: 10.1039/x0xx00000x

www.rsc.org/

Six new 2, 4-linked *exo/endo* sesquiterpene lactone dimers, faberidilactones A–E (1–5) and endodischkuhriolin (6), were isolated from *Carpesium faberi*. The characteristic chemical shift of Ha-3' and diagnostic negative/positive CE can be used to assign the *exo/endo* stereochemistry of those dimers. Compounds 1–3, 5 and 6 exhibited potent cytotoxicity with IC₅₀ value in the range of 1.11–8.50 μ M against the four human tumor cell lines (CCRF-CEM, K562, HL-60 and HCT116 cells). Moreover, 1, 3 and 5 (*exo*-SLDs) showed potent NF- κ B inhibitory effect with inhibition ratio of 65.98, 53.27 and 71.45 %, respectively.

Sesquiterpene lactone dimers (SLDs) represent the class of natural products that have C₃₀ framework biosynthetically derived from two homo or hetero sesquiterpene monomers.¹ Most of them were formed by biosynthetic Diels-Alder [4+2] cycloaddition, exhibiting region/stereo selectivity. Since the first SLD Absinthin was isolated from *Artemisia absinthium* in 1950s, more than 150 SLDs have been discovered from the family Compositae. Their diverse skeletons, complex stereochemistry and potent antitumor activity have drawn the attention of chemists and pharmacologists.^{1–4}

Structurally, the region/stereo selective SLDs can also be classified into several subclasses according to their linkages, such as 2, 4/-1, 3/-1, 4-linked SLDs. Before our investigation, there were four 2, 4-linked SLDs isolated from the family Compositae, but only one of them, dischkuhriolin,⁵ was unambiguously elucidated as an *exo*-SLD *via* X-ray crystallographic data. An overview of reports on the structure elucidation of these Diels-Alder adducts revealed that it was a hard work to resolve the relative and absolute configuration of the three newly formed stereogenic centers of C-11, C-2' and

C-4' (or namely *exo/endo* orientation), due to the lack of sufficient NOESY correlations and suitable crystals for X-ray single crystal diffraction.^{6–8}

In our previous works, three 2, 4-linked *exo*-type eudesmanolide-guaianolide SLDs, carpedilactones A–C, were isolated from the title plant, and their absolute configuration were also determined by Cu-K α X-ray crystallographic analysis.⁹ Since the corresponding 2, 4-linked *endo*-type SLDs were never obtained from nature, it's difficult to summarize the spectral difference between the *exo* and *endo* SLDs. Fortunately, in our continuing work, a pair of 2, 4-linked *exo/endo* diastereoisomeric carabranolide-guaianolide dimers and three *exo* congeners, faberidilactones A–E (1–5), together with endodischkuhriolin (6), the *endo* diastereoisomer of dischkuhriolin⁵ (Fig. 1), were isolated from the same plant. Compounds 1–5 are the first five SLDs with new carabranolide-guaianolide skeleton formed by the enzymatic Diels-Alder [4+2] addition.^{9,10} Furthermore, detailed analysis of the spectra of 1–6 led to the findings of two spectrographic features: the characteristic chemical shift of Ha-3' and diagnostic negative/positive Cotton effect (CE), which can be simply used to elucidate the *exo/endo* configuration of those 2, 4-linked SLDs. Herein, we described the isolation, structure elucidation and NF- κ B inhibitory activity of 1–6.

Faberidilactone A (1), isolated as an optically active colourless oil with $[\alpha]_D^{25} +40.4$ (c 1.288, CH₃OH), was

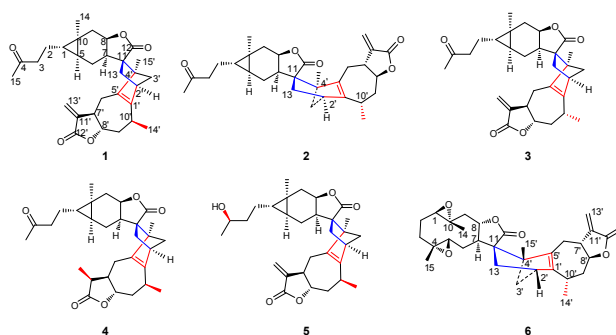


Fig. 1 Chemical structures of 1–6.

^a Department of Phytochemistry, School of Pharmacy, Second Military Medical University, Shanghai 200433, P. R. China. faranli@hotmail.com, wdzhangy@hotmail.com

^b School of Pharmacy, East China University of Science and Technology, Shanghai 200237, P. R. China

^c Shanghai Institute of Pharmaceutical Industry, Shanghai 200040, P. R. China

[†] Electronic Supplementary Information (ESI) available: The extraction scheme, compounds characterization, spectroscopic data, bioassay methods, computational method, and crystallographic data of 6. See DOI: 10.1039/x0xx00000x

preliminarily determined as a dimeric sesquiterpene lactone, based on the molecular formula $C_{30}H_{38}O_5$ (HRESIMS at m/z 479.2833 $[M + H]^+$, calcd 479.2792) and typical 1H and ^{13}C NMR signals for SLDs (Tables S1 and S2, ESI[†]), including one α -methylene- γ -lactone functionality (δ_H 6.11, d, $J=3.5$ Hz, Ha-13'; δ_H 5.69, d, $J=3.5$ Hz, Hb-13'; δ_C 171.8/119.8, C-12'/13'), one downfield shifted signal of carbonyl group of lactone (δ_C 184.0, C-12), and two characteristic oxygenated CH of lactone (δ_H 4.83, m, H-8; 4.32, m, H-8'; δ_C 77.4, C-8; 83.0, C-8').

Comprehensive NMR analysis resulted in the assembly of two subunits A and B. Unit A was assigned as a carabrone moiety¹¹ due to the four typical multiplets in the most upfield region: δ_H 0.30 (1H, m, H-5), 0.43 (1H, m, H-1), 0.66 (1H, m, Hb-6), 0.88 (1H, m, Hb-9), as well as the characteristic signals for a CH_3CO - group at δ_H 2.13 (3H, s, H₃-15)/ δ_C 30.0 (C-15), 211.5 (C-4). Further evidences come from 2D NMR analysis. A proton-bearing structural fragment of H₂-3/H₂-2/H-1/H-5/H₂-6/H-7/H-8/H₂-9 was constructed by analysis of the 1H - 1H COSY and HSQC-TOCSY experiments (Fig. 2). The HMBC correlations of H-1/C-2, C-3 and C-10; of H-5/C-1, C-2, C-10 and C-14; of H-7/C-6, C-8, C-11 and C-12; of H-8/C-6, C-9 and C-12; of H₂-13/C-11 and C-12; of H₃-14/C-1, C-5, C-9 and C-10; of H₃-15/C-4 and C-3 were observed in HMBC spectrum (Fig. 2). Similarly, the unit B was established as a guaianolide moiety according to the long proton-proton correlations system H₂-6'/H-7'/H-8'/H₂-9'/H-10'/H₃-14' in 1H - 1H COSY and HSQC-TOCSY spectra, combined with the key HMBC correlations of H-2'/C-4', C-5' and C-10'; of H-7'/C-8', C-9' and C-11'; of H-8'/C-6' and C-10'; of H₂-13'/C-7', C-11' and C-12'; of H₃-14'/C-1', C-9' and C-10'; of H₃-15'/C-3', C-4' and C-5' (Fig. 2). Therefore, compound **1** was proposed to be formed by a carabrone and a guaianolide.

The linkage of the two units *via* two C-C single bonds between C-13/C-2' and C-11/C-4' was deduced from the 1H - 1H COSY correlations of H₂-13/H-2'/H₂-3', and the key HMBC correlations of H-2'/C-13; of H₃-15'/C-11; of H₂-13/C-1', C-2' and C-3' (Fig. 2). Thus, the planar structure of **1** was constructed as shown in Fig. 2, probably formed from a Diels-Alder [4+2] cycloaddition of the carabrone unit as the dienophile and the guaianolide unit as the diene.

The relative configuration of asymmetry carbons in **1** was concluded from the NOESY correlations. In unit A, the H-7 was arbitrarily assigned as the α -orientation under the biogenetic consideration, then the key NOESY correlations of H-7/H-8/H₃-14/H-5/H₂-2, but not with H-1 (Fig. 2), indicated that H-7, H-8, H₃-14, H-5 and H₂-2 were in the same face and were assigned as α -orientation, while H-1 was assigned as β -orientation, in agreement with those of carabrone. In unit B, the NOESY

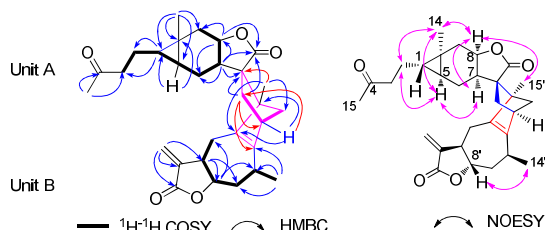


Fig. 2 Selected NMR correlations of **1**.

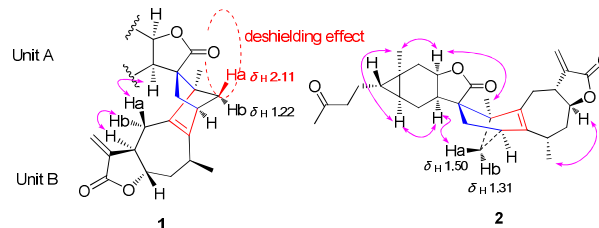


Fig. 3 Selected NOESY correlations () of **1** and **2**, and the deshielding effect of carbonyl group of C-12.

correlation of H-8' with H₃-14', but not with H-7' (Fig. 2), showed that H-8' and H₃-14' were in the same face, while H-7' was at the opposite side. Particularly, the relative configuration of the spiro-atom C-11 was resolved through the key NOESY correlation of H-8/H₃-15' (Fig. 2), suggesting that the CH₂-13 should be β -oriented. Meanwhile, the key NOESY correlations of Ha-6'/H-7; of Hb-6'/H-7' (Fig. 3) were found out, indicating that **1** was a stacked arrangement of two sesquiterpene monomers (i. e., *exo* orientation) (Fig. 3).

Interestingly, faberidilactone B (**2**), an *endo* diastereoisomer of **1**, was co-isolated from the same plant. **2** was an optically active colourless oil with $[\alpha]_D^{25} +124.3$ (c 0.05, CH₃OH). HRESIMS data at m/z 501.2591 ($[M+Na]^+$, calcd 501.2611) of **2** implied its molecular formula was $C_{30}H_{38}O_5$, same as that of **1**. Detailed 1D and 2D NMR analysis indicated that **2** had the same planar structure as **1** (Tables S1 and S2, ESI[†]). In addition, the relative configuration of C-11 was also resolved by the NOESY correlation of H-8/H₃-15' (Fig. 3), exhibiting that the CH₂-13 was β -oriented. Differently, the key NOESY correlation of Ha-3'/H-7 (Fig. 3) showed that **2** was the stretched arrangement between two monomers, and **2** must be the *endo* diastereoisomer of **1**.

Inspecting the differences between **1** and **2** on 1H NMR data (Tables S1 and S2, ESI[†]), we found the most obvious change was the chemical shift of Ha-3', i. e., the chemical shift of Ha-3' was upfield shifted from δ_H 2.11 in **1** to δ_H 1.50 in **2** (Fig. 3), indicating that the downfield chemical shift of Ha-3' in **1** was the result of the deshielding effect of carbonyl at C-12. Thus, the structures of **1** and **2** were established as shown in Fig. 3.

In order to solve the absolute configuration of **1** and **2**, a theoretical calculation of their electronic circular dichroism (ECD) spectra was performed using time-dependent density-functional theory (TD-DFT) at the B3LYP/TZVP level with the PCM model in methanol solution (ESI[†]). As shown in Fig. 4, the ECD spectra of model A and model B were well in accordance with the experimental CD spectrum of **1** and **2**, respectively. Subsequently, the absolute configuration of **1** was assigned as 1*S*, 5*S*, 7*R*, 8*R*, 10*R*, 11*S*, 2'*S*, 4'*R*, 7'*R*, 8'*S*, 10'*S*. Differently, the chirality of C-2' and C-4' in **2** were assigned as 2'*R*, 4'*S*.

Obviously, the *exo*-SLDs (**1**, **3**–**5** and carpedilactones A–C⁹) (Their CD spectra attached in ESI[†]) showed an intense negative CE around 214 nm, while the *endo*-SLDs **2** and **6** showed an intense positive CE around 228 nm (Fig. 4 and ESI[†]), demonstrating that the conformationally flexible side chain at C-1, the carbonyl chromophore at C-4 and the double bond between C-11' and C-13' had hardly any effect on their spectra,

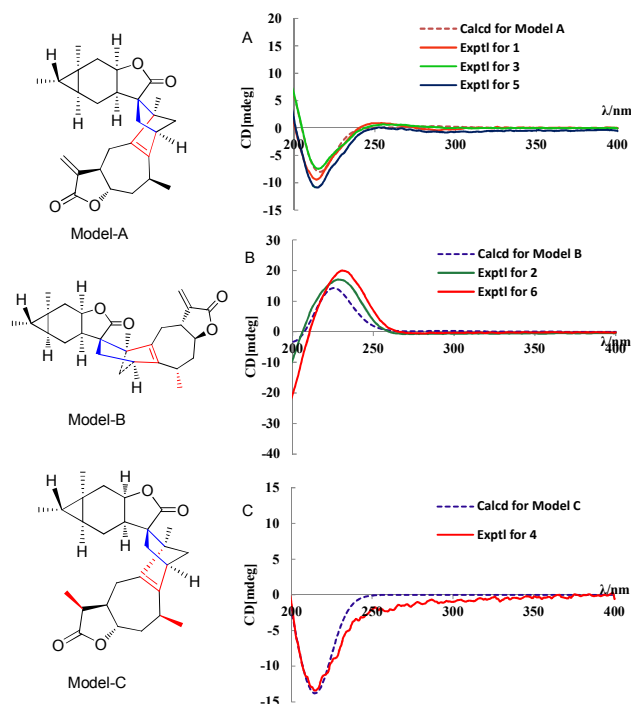


Fig. 4 Model-A (simplified model structure of **1**, **3** and **5**), Model-B (simplified model structure of **2**), and Model-C (simplified model structure of **4**) in which the butan-2-one or the butan-2-ol side-chain were replaced by a methyl group, respectively, since these side-chain contribute only weakly to the observed CD spectra of compounds **1–5**; (A) Calculated and experimental ECD spectra of **1**, **3** and **5**. (B) Calculated and experimental ECD spectra of **2** and **6**. (C) Calculated and experimental ECD spectra of **4**.

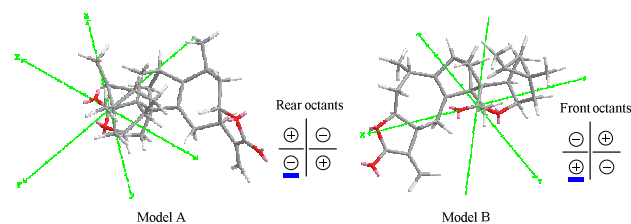


Fig. 5 Model A and Model B viewed along the O=C bond on axes as employed in application of the octant rule.

which agreed with the theoretical basis that only if the strongly absorbing chromophores located near in space and close in energy, very intense CD couplets would be arose.^{12,13} Thus, we deduced that their opposite CE was only associated with the isolated carbonyl chromophore at C-12, i. e., other chromophores did not participate at all in the chromophoric systems, so their opposite CE could be successfully explained by the ketone octant rule¹².

As shown in Fig. 5, it is apparent that the contribution of all atoms and groups nearly cancel each other with the exception of the unit B. The unit B of Model A in bottom left corner in rear octants justified the negative sign observed in the CD spectrum, on the contrary, the unit B of Model B in bottom left corner in front octants confirmed the positive sign observed in the CD spectrum. Hence, the CD spectrum of **2**, 4-linked SLDs is an extraordinary reporter of the exo/endo configuration.

Faberidilactone C (**3**), was isolated as an optically active

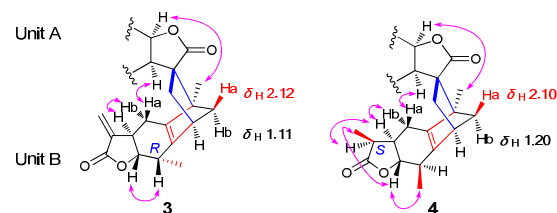


Fig. 6 Selected NOESY correlations () of **3** and **4**.

colourless oil with $[\alpha]_D^{25} +38.0$ (c 0.05, CH₃OH). From the observation of 1D and 2D NMR spectra of **3** (Tables S1 and S2, ESI[†]), it was discovered that the chemical structure of **3** was the epimer of **1** at C-10', which were supported by the NOESY correlation of H-10'/H-8' (Fig. 6). Therefore, the absolute configuration of C-10' was confirmed as *R*.

Faberidilactone D (**4**), was isolated as a colourless oil with $[\alpha]_D^{25} -0.56$ (c 0.3, CH₃OH). The positive HRESIMS at m/z 481.2985 ($[M+H]^+$, calcd 481.2949) of **4** indicated a molecular formula of C₃₀H₄₀O₅, which was two hydrogen atoms more than that of **1**. The H₂-13' was disappeared and an additional doublet methyl was present in ¹H NMR spectra (Tables S1 and S2, ESI[†]), required that the $\Delta^{11'(13')}$ exocyclic double bond was reduced to the methyl. This interpretation was also supported by the HMBC correlations of H₃-13' with C-11', C-12' and C-7' (Fig. 6). Furthermore, the relative configuration of CH₃-13' was elucidated as β -orientation by the key NOESY correlations of H₃-13' with H-8' and of H-11' with H-7' (Fig. 6). Thus, the absolute configuration of C-11' was determined as *S*.

Faberidilactone E (**5**), isolated as an optically active colourless oil with $[\alpha]_D^{25} +54.3$ (c 0.077, CH₃OH). The HRESIMS and NMR spectra of **1** and **5** (Tables S1 and S2, ESI[†]) suggested that these two compounds are a keto-nealcohol pair, which were supported by the following evidences: (1) the carbonyl of ketone at δ_C 211.5 in **1** was replaced by the oxygenated methine at δ_C/δ_H 68.3/3.72 in **5**; (2) the singlet acetyl methyl at δ_H 2.13 (s, H₃-15) in **1** transferred to the doublet methyl at δ_H 1.14 (d, H₃-15) in **5**; (3) the ¹H-¹H COSY correlations of H₃-15/H-4/H₂-3/H₂-2/H-1 in **5**; (4) the HMBC correlations of H₃-15 with H-4 and H-3 in **5**, revealing that the carabrone moiety (unit A) has changed to carabrol.¹⁴ Subsequently, the *R*-configuration of C-4 was confirmed by the modified Mosher's method (Fig. 7, ESI[†]).¹⁵

Although the NMR data of endodischkuhriolin (**6**) (Tables S1 and S2, ESI[†]) was closely similar to dischkuhriolin⁵, there were some obvious differences, i. e., in ¹H NMR, the upfield chemical shift of Ha-3' at δ_H 1.47 in **6**, in contrast to that of Ha-3' (δ_H 2.46) in dischkuhriolin; in NOESY, the correlation of

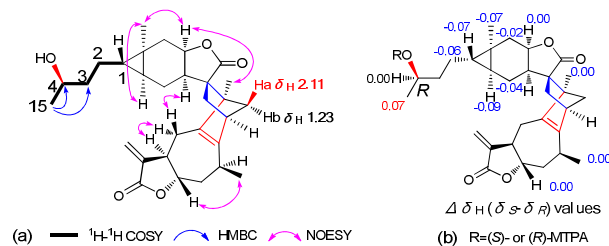


Fig. 7 (a) Selected NMR correlations of **5**. (b) $\Delta\delta_H$ ($\delta_S - \delta_R$) values obtained for the MTPA esters of **5**.

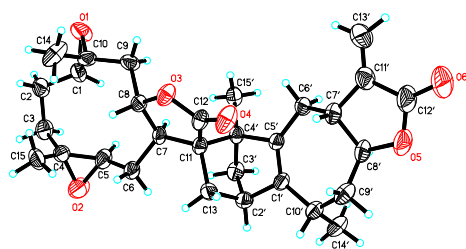


Fig. 8 X-ray crystallographic structure of **6**.

H-7/Ha-3' was observed in **6**, instead of the correlation of H-5/H-8' in dischkuhriolin, revealing that **6** was the endo-type diastereoisomer of dischkuhriolin. For unambiguous confirmation of the stereochemical structure of **6**, a single-crystal X-ray diffraction experiment was performed, and the absolute configuration was assigned as 1*R*, 4*R*, 5*R*, 7*R*, 8*S*, 10*R*, 11*S*, 2'*R*, 4'*S*, 7'*R*, 8'*S*, 10'*S* (Fig. 8, CCDC-1035615, ESI[†]), which confirmed our above deduction.

Compounds **1–3**, **5** and **6** were found to be cytotoxic against the four cell lines (CCRF-CEM, K562, HL-60 and HCT116 cells) with IC₅₀ value in the range of 1.11–8.50 μM, which better than that of the dimer without α-methylene-γ-lactone **4** and the two monomers carabrone **7** and 4*R*-carabrol **8** (Table S3, ESI[†]). Mechanism studies¹⁶ showed that the three exo-SLDs **1**, **3** and **5** had potent NF-κB inhibitory activity with inhibition ratio of 65.98, 53.27 and 71.45 %, respectively, which stronger than that of the endo-SLD **2** with inhibition ratio of 38.59 %. Furthermore, **1**, **3** and **5** dose-dependently suppressed TNF-α-induced phosphorylation of the NF-κB p65 subunit and degradation of IκBα in bEnd.3 cells (Fig. 9A–9D, ESI[†]). These above data indicated that: (1) the cytotoxicity of the SLDs **1–3** and **5** was attributed to the function of α-methylene-γ-lactone acting as alkylating agent and dimerization; (2) **1**, **3** and **5** (exo-SLDs)-induced cytotoxicity might be attributed to suppressing NF-κB activation, while the endo-SLD **2** might not be restricted to this mechanism of action.

In conclusion, six new 2, 4-linked SLDs, faberidilactones A–E (**1–5**) and endodischkuhriolin (**6**), were isolated from

Carpesium faberi. Notably, the spectrographic results of **1–6**, dischkuhriolin⁵ and carpedilactones A–C⁹ discovered that the 2, 4-linked exo-SLD was the stacked arrangement of two monomers, whereas the endo SLD was the stretched arrangement between two monomers, as well as their two spectrographic features. Meanwhile, we believed that the two features could be applied to the determination of exo/endo stereochemistry of 1, 3-linked SLDs, since they possess the similar exo/endo norbornylene core scaffold and the same carbonyl chromophore at C-12.

The work was supported by program NCET Foundation, NSFC (81102335, 81473109), National High-Tech Research and Development Program of China (863 Program, 2014AA022201-03), Shanghai Leading Academic Discipline Project (B906), Key laboratory of drug research for special environments, PLA, Shanghai Engineering Research Center for the Preparation of Bioactive Natural Products (10DZ2251300), the Scientific Foundation of Shanghai China (12401900801, 13401900101), National Major Project of China (2014ZX09101003-001), the National Key Technology R&D Program of China (2012BAI29B06) and China Postdoctoral Science Foundation funded project.

Notes and references

- Z.-J. Zhan, Y.-M. Ying, L.-F. Ma and W.-G. Shan, *Nat. Prod. Rep.*, 2011, **28**, 594–629.
- E. M. Stocking and R. M. Williams, *Angew. Chem. Int. Ed.*, 2003, **42**, 3078–3115.
- C. Li, X.-L. Yu and X.-G. Lei, *Org. Lett.*, 2010, **12**, 4284–4287.
- T. Dong, C. Li, X. Wang, L.-Y. Dian, X.-G. Zhang, L. Li, S. Chen, R. Cao, L. Li, N. Huang, S.-D. He and X.-G. Lei, *Nat. Commun.*, 2015, **6**, 1–12.
- A. León, B. M. Reyes, M. I. Chávez, R. A. Toscano and G. Delgado, *J. Mex. Chem. Soc.*, 2009, **53**, 193–200.
- A. Ovezdurdyev, N. D. Abdullaev, M. I. Yusupov and S. Z. Kasymov, *Chem. Nat. Compd.*, 1987, **23**, 553–556.
- J. Jakupovic, C. Zdero, M. Grenz, F. Tschritzis, L. Lehmann, S. M. Hashemi-Nejad and F. Bohlmann, *Phytochemistry*, 1989, **28**, 1119–1131.
- A. Trendafilova, M. Todorova, B. Mikhova, A. Vitkova and H. Duddeck, *Phytochemistry*, 2006, **67**, 764–770.
- Y.-X. Yang, L. Shan, Q.-X. Liu, Y.-H. Shen, J.-P. Zhang, J. Ye, X.-K. Xu, H.-L. Li and W.-D. Zhang, *Org. Lett.*, 2014, **16**, 4216–4219.
- K. Alder and G. Stein, *Justus Liebigs Ann. Chem.* 1934, **514**, 1–33.
- M. Maruyama and S. Omura, *Phytochemistry*, 1977, **16**, 782–783.
- N. Berova, L. D. Bari and G. Pescitelli, *Chem. Soc. Rev.*, 2007, **36**, 914–931.
- J.-J. Qin, L.-Y. Wang, J.-X. Zhu, H.-Z. Jin, J.-J. Fu, X.-F. Liu, H.-L. Li and W.-D. Zhang, *Chem. Commun.*, 2011, **47**, 1222–1224.
- M. Maruyama, A. Karube and K. Sato, *Phytochemistry*, 1983, **22**, 2773–2774.
- I. Ohtani, T. Kusumi, Y. Kashman and H. Kakisawa, *J. Am. Chem. Soc.*, 1991, **113**, 4092–4096.
- L. Liu, Y.-P. Hua, D. Wang, L. Shan, Y. Zhang, J.-S. Zhu, H.-Z. Jin, H.-L. Li, Z.-L. Hu and W.-D. Zhang, *Chem. Biol.*, 2014, **21**, 1–10.

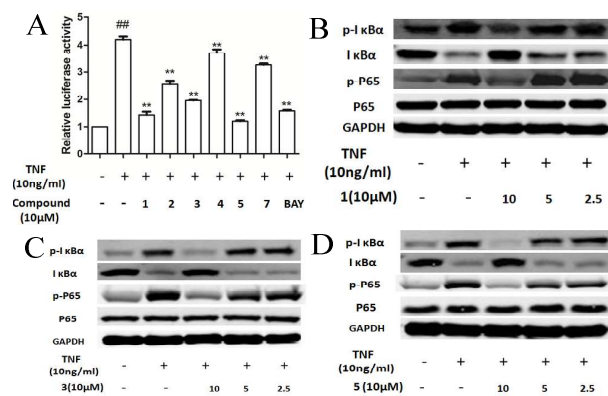


Fig. 9 (A) Compounds **1–5** and **7** inhibited TNF-α-induced NF-κB activation. ## *p* < 0.01, relative to control group; ** *p* < 0.01, relative to TNF-α treatment group. (B–D) Compounds **1**, **3** and **5** (2.5–10 μM) dose-dependently suppressed TNF-α-induced phosphorylation of the NF-κB p65 subunit and degradation of IκBα in bEnd.3 cells.